AIP | The Journal of Chemical Physics

The effect of classical and quantum dynamics on vibrational frequency shifts of H2 in clathrate hydrates

Nuria Plattner and Markus Meuwly

Citation: The Journal of Chemical Physics **140**, 024311 (2014); doi: 10.1063/1.4859856
View online: http://dx.doi.org/10.1063/1.4859856
View Table of Contents: http://scitation.aip.org/content/aip/journal/jcp/140/2?ver=pdfcov
Published by the AIP Publishing

The effect of classical and quantum dynamics on vibrational frequency shifts of H_2 in clathrate hydrates

Nuria Plattner[1,a] and Markus Meuwly[2,b]
[1]*Department of Mathematics and Computer Science, Free University Berlin, Arnimallee 6, 14195 Berlin, Germany*
[2]*Department of Chemistry, University of Basel, Klingelbergstrasse 80, CH-4056 Basel, Switzerland and Chemistry Department, Brown University, Providence, Rhode Island 02912, USA*

(Received 3 May 2013; accepted 5 December 2013; published online 13 January 2014)

Vibrational frequency shifts of H_2 in clathrate hydrates are important to understand the properties and elucidate details of the clathrate structure. Experimental spectra of H_2 in clathrate hydrates have been measured for different clathrate compositions, temperatures, and pressures. In order to establish reliable relationships between the clathrate structure, dynamics, and observed frequencies, calculations of vibrational frequency shifts in different clathrate environments are required. In this study, a combination of classical molecular dynamics simulations, electronic structure calculations, and quantum dynamical simulation is used to calculate relative vibrational frequencies of H_2 in clathrate hydrates. This approach allows us to assess dynamical effects and simulate the change of vibrational frequencies with temperature and pressure. The frequency distributions of the H_2 vibrations in the different clathrate cage types agree favorably with experiment. Also, the simulations demonstrate that H_2 in the 5^{12} cage is more sensitive to the details of the environment and to quantum dynamical effects, in particular when the cage is doubly occupied. We show that for the 5^{12} cage quantum effects lead to frequency increases and double occupation is unlikely. This is different for the $5^{12}6^4$ cages for which higher occupation numbers than one H_2 per cage are likely. © *2014 AIP Publishing LLC*. [http://dx.doi.org/10.1063/1.4859856]

I. INTRODUCTION

Hydrogen clathrate hydrates are ice-like materials with hydrogen molecules occupying cages formed by water molecules. Due to their high H_2-storage capacity, the usefulness of clathrate hydrates as a hydrogen storage material has been investigated and it has been found that the stability of hydrogen clathrates can be tuned by combining hydrogen with other guest molecules.[1] The structure of hydrogen clathrates has been determined to be clathrate type II.[2] The clathrate type II unit cell consists of 136 water molecules which form 8 large and 16 small clathrate cages. The small clathrate cages consist of pentagonal water clusters forming a pentagonal dodecahedron (5^{12}), while the large cages are composed of pentagonal and hexagonal ($5^{12}6^4$) water clusters.[3] Ratios of up to 1:2 H_2:H_2O are known to be stable, but the occupancy of the individual cages is not straightforward to determine. Varying occupation numbers of the two clathrate cage types have been related to various properties of hydrogen clathrates such as the stability of the clathrate at different temperatures and pressures, the change in stability upon combination of H_2 with other guest molecules, and the vibrational frequency shifts of H_2 in different clathrate environments compared to free H_2.[1,2,4–7] Vibrational spectra of H_2 in clathrate hydrates have been experimentally determined for a range of clathrate compositions at different temperatures and pressures.[2,5–7]

Vibrational frequencies are a sensitive probe of the molecular environment and are affected by both, structural and dynamical effects. For clathrate hydrates it has been found that the vibrational frequency shift of H_2 molecules in the different clathrate cage types compared to free H_2 depends on the clathrate composition, pressure, and temperature.[2,5] In general the H_2 frequencies in clathrate hydrates are redshifted compared to free H_2, which is in contrast to other H_2O-ice environments where blueshifted H_2 frequencies are found.[8] Due to symmetry constraints, hydrogen exists as *ortho* and *para* hydrogen, with an *ortho*:*para* ratio of 3:1 at high temperatures. For the interpretation of H_2 Raman spectra, the existence of these two H_2 forms needs to be taken into account, mainly because the two forms exist in specific rotational states.[5,7] The frequency shifts of H_2 in clathrate hydrates have therefore to be evaluated by comparing either the *ortho* or the *para* hydrogen frequencies in different environments in order to distinguish the environment dependent frequency shifts from the differences between the rotational states. For hydrogen clathrates at 76 K and 100 bars, three distinct hydrogen environments have been observed with vibrational frequency shifts of about -35, -15, and -10 cm^{-1} compared to the vibrational frequency of free H_2 at 4155 cm^{-1}. For tetrahydrofuran-H_2 clathrate at 100 bars and 296 K, a redshift of about -35 cm^{-1} is observed.[7] The different frequency shifts are attributed to H_2 positions in varying clathrate cages and to different numbers of hydrogen molecules per cage. The pressure dependence of the frequency shift is also attributed to different cage occupancies.[6] Experiments with tetrahydrofuran clathrates established that the most redshifted features in

[a]Electronic mail: nuria.plattner@fu-berlin.de
[b]Electronic mail: m.meuwly@unibas.ch

the Raman spectra correspond to H_2 positions in the 5^{12} cage.[9] However, a direct relationship between spectral patterns (e.g., frequency shifts) and structure is not straightforward to establish from experiment alone because such studies would need to be carried out simultaneously as has been done for CO-stretching frequencies in myoglobin.[10] Atomistic simulations with accurate force fields have been used successfully to interpret experimental spectra and establish relationships between structures and spectroscopic features.[11–13]

The potential cage occupancies have been investigated by experiment and theory in the past, with the major uncertainty being the occupancy of the 5^{12} cages.[2,4,14–16] Vibrational frequency shifts are one of the major sources of information about the cage occupancies due to their dependence on the local environment. In order to use the information contained in experimentally observed H_2 frequency shifts, a relationship between these frequency shifts and structural and dynamical properties of hydrogen clathrates needs to be established. For this purpose, a reliable calculation of the vibrational frequency shifts is required. Calculating the vibrational frequencies of H_2 in clathrates accurately is however difficult due to the following reasons:

- The system size required for a realistic simulation should be sufficiently large, including about 1000 water molecules and several 100 H_2 molecules. The use of empirical force fields is therefore necessary.
- The calculation of vibrational frequencies and frequency shifts requires a reliable potential function, therefore the force field simulation needs to be combined with an electronic structure calculation method or with force fields capable of accurately determining vibrational frequencies.
- Due to the low temperatures at which experiments are typically carried out and the importance of hydrogen atom motion in the system, quantum dynamical effects may play an important role.

These aspects need to be considered in the interpretation of vibrational frequency calculations. High level quantum mechanical calculations have been carried out for H_2 in different clathrate cages.[17–20] These calculations provide a basis for comparing the energies of H_2 in different clathrate environments, but did not report any actual frequencies. In combination with the loose cage-tight cage model,[21] interaction energy curves of guest molecules with the clathrate lattice have been used successfully to assess frequency shifts in clathrate hydrates with different guest molecules.[22] Density functional theory (DFT) has been used to calculate the vibrational frequencies of methane and H_2 in clathrate hydrates.[23,24] However, the system size and number of clathrate conformations which can be included in DFT studies with a reasonable computational effort is too small to extensively sample the conformational space of sufficiently large periodic clathrate systems and assess the effect of different clathrate conformations on the frequency shifts. In order to address this problem, DFT has been combined with empirical force fields for the calculation of the frequency shifts.[16] Based on the coordinates from molecular dynamics (MD) simulations, structures of hydrogen containing clathrate cages were optimized using DFT calculations and harmonic frequencies were calculated based on these optimized structures.[16] However, frequency calculations on optimized structures do not include temperature effects. Furthermore, no quantum dynamical effects were taken into account in these calculations. The importance of quantum dynamical effects for hydrogen clathrates has been demonstrated in other studies based on analyses of structural properties.[15,25]

In the present study, a combination of complementary simulation strategies is used to calculate relative vibrational frequency shifts of hydrogen in clathrate hydrates and to assess the order of magnitude of temperature and quantum dynamical effects on the spectra. The calculations are further validated by comparing force field parametrizations and electronic structure calculations at different levels of sophistication. Atomistic MD simulations with atomic multipole moments are carried out on a periodic clathrate system of $2 \times 2 \times 2$ hydrogen clathrate unit cells with different amounts of hydrogen and at different temperatures and pressures. The importance of accurate force fields and the usefulness of atomic multipole moments for the calculation of vibrational spectra have been demonstrated in previous studies for clathrate hydrates and amorphous ices.[12,26–28] For the calculation of the vibrational frequencies, the atomistic MD simulations are combined with electronic structure calculations using DFT and MP2 methods. In order to include quantum dynamical effects, path integral MD (PIMD) simulations are carried out on a clathrate model system and the results are compared with the classical simulations and with experiment.

II. COMPUTATIONAL METHODS

The clathrate structure was generated as follows: Based on the X-ray structure oxygen positions for clathrate type II,[2] water hydrogen atoms were added. The positions of the water hydrogens were then iteratively optimized by several energy minimizations and simulated annealing dynamics at low temperatures. After the optimization, the hydrogen atom positions were consistent with the ice rules. To obtain initial positions for the H_2 molecules, a box of 432 H_2 molecules was first equilibrated at 150 K and 200 bars for 100 ps in the *NPT* ensemble, leading to a box size of $18 \times 18 \times 18$ Å, close to the volume of the clathrate unit cell ($17 \times 17 \times 17$ Å). Hydrogen and clathrate unit cells were then superimposed and overlapping hydrogens deleted, with the radius of overlap to the oxygen atoms such that a H_2:H_2O ratio of about 1:2 was obtained.

Periodic systems: A larger system of $2 \times 2 \times 2$ unit cells was generated based on the initial unit cell. The system contained 1088 water molecules and 624 hydrogens, i.e., 57.35% of hydrogen by number. Based on this initial hydrogen load, four systems with lower hydrogen loads were generated by deleting hydrogens within different radii of water in the optimized structures. The four systems contain 575, 456, 313, and 144 hydrogen molecules, corresponding to 52.85%, 41.91%, 28,77%, and 10.48% of hydrogen. The system with the highest H_2 fraction is shown in Figure 1. With this setup, the occupancy numbers are allowed to vary slightly for different cages within a given system, which is also what may happen in

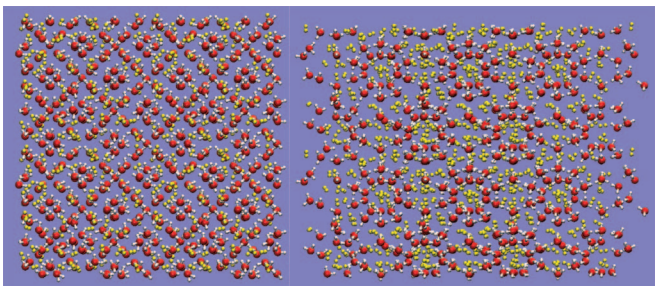

FIG. 1. Optimized structure of periodic system with highest hydrogen load (57.35%). Hydrogen molecules are shown in yellow. The structure on the left hand side is viewed along the (100) and the structure on the right hand side is viewed along the (110) face.

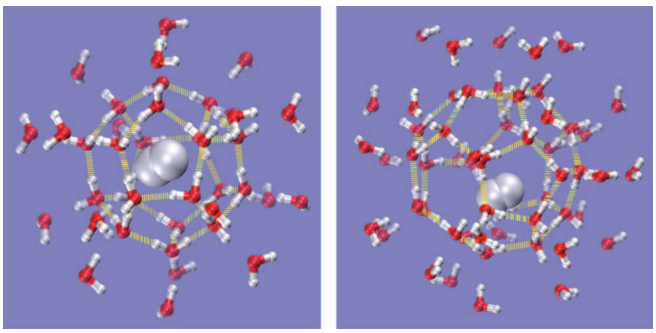

FIG. 2. Hydrogen clathrate model system for the 5^{12} cage (left) and the $5^{12}6^4$ cage (right) shown with one hydrogen molecule. Hydrogen bonds are represented by yellow lines for the inner layer of water molecules in each cage.

experiments where the occupancy is only controlled by the hydrogen pressure. During the equilibration phase of the simulations the occupation numbers between different cages tend to equilibrate rather rapidly, i.e., H_2 molecules diffuse from cages with higher occupancies to cages with lower occupancies and therefore the occupancies tend to be equal.

Model systems: Based on the water coordinates of the periodic systems, model systems for the 5^{12} and the $5^{12}6^4$ clathrate cage were generated. The model system for the 5^{12} cage contains 40 water molecules arranged in two layers. The inner layer is composed of 20 waters and forms a cluster which corresponds to a 5^{12} cage. The outer layer consists of the next neighboring waters for each of the inner layer waters. For the $5^{12}6^4$ clathrate cage, each layer is composed of 28 water molecules. During the simulations, a harmonic constraint is applied to the oxygen atoms in the outer layer. The H_2 occupation for the 5^{12} cage model is one and two, whereas for the $5^{12}6^4$ cage up to four hydrogens are used. The two model systems are shown in Figure 2.

A. Force field parameters and potentials

All simulations were carried out with the CHARMM program[29,30] with provisions for evaluating electrostatic interactions involving atomic multipole moments, a modified Lennard-Jones (LJ) potential for the H_2-H_2 interaction and anharmonic bond potentials for H_2 and water. The additional interaction terms and parameters are discussed in this section.

Electrostatic interactions are described by atomic multipole moments based on the distributed multipole analysis (DMA).[31,32] Two sets of parameters for water and H_2 multipole moments up to quadrupole were obtained based on B3LYP/6-31G* and MP2/6-31G* calculations using GAUSSIAN.[33] These choices are based on previous experience in the performance of these methods[12,26–28] and the fact that electronic structure calculations for the vibrational frequencies of a system containing up to 58 water and up to 4 H_2 molecules are also possible at this level of theory. The multipole parameters are reported in Tables I and II.

For the water molecules the TIP3P LJ parameters[34] were used without further refinement since the water-water interaction is dominated by electrostatic terms and therefore changes in the LJ parameters contribute only very little to the overall interaction energy. For H_2 in contrast, the LJ parameters are important because the electrostatic part of the interaction is weak. Therefore, LJ parameters were fitted for each set of electrostatic parameters based on the interaction energy of the underlying electronic structure calculation method. Parameters were fitted for the H_2-water and H_2-H_2 interaction separately. For H_2-water, the LJ 6-12 potential provided in the standard CHARMM force field was used. For H_2-H_2, the standard potential was replaced by a LJ 9-10 potential of the form

$$V_{LJ} = \varepsilon\left(\left(\frac{\sigma}{r_{\text{cent}}}\right)^{10} - \left(\frac{\sigma}{r_{\text{cent}}}\right)^{9}\right), \tag{1}$$

where ε and σ are the fitted parameters and r_{cent} is the distance between the geometric centers of the given H_2 molecules. The (9,10) exponents were found to be more suitable to describe the H_2-H_2 interaction and this is consistent with recent detailed investigations of interaction energies using multipolar force fields,[35] which confirm previous studies stating that the (6,12) LJ potential should be replaced by other LJ potential forms to better reproduce interaction energies.[36,37] Geometries for reference energies included 1000 random configurations of the water-H_2 and H_2-H_2 dimer. It should be noted that

TABLE I. Atomic multipole moments in spherical tensor notation[31,32] for water calculated at different levels of theory.

			Dipole (ea_0)	Quadrupole (ea_0^2)	
		Charge (e)	$q10$	$q20$	$q22c$
B3LYP/6-31G*	Oxygen	−0.469056	−0.293739	0.076588	−1.036956
B3LYP/6-31G*	Hydrogen	0.234528	...	...	...
MP2/6-31G*	Oxygen	−0.480928	−0.323179	0.081444	−1.126157
MP2/6-31G*	Hydrogen	0.240464	...	...	...

TABLE II. Atomic multipole moments in spherical tensor notation[31,32] for H_2 at different levels of theory.

		Dipole (ea_0)	Quadrupole (ea_0^2)
		$q10$	$q20$
B3LYP/6-31G*	Hydrogen	−0.089557[a]	0.283542
MP2/6-31G*	Hydrogen	−0.095760[a]	0.285438

[a]Opposite signs on the two hydrogens.

the configurations were generated in the entire configuration space, not within a linear or otherwise idealized configuration subset. The interaction energy was calculated for each of the configurations using the same two electronic structure calculation methods as for the parametrization of the electrostatic potential. Counterpoise corrections were used to account for the basis set superposition error.[33,38] From this overall interaction energy of each pair of molecules, the electrostatic interaction energies calculated from the multipole moments of the corresponding method were subtracted. LJ parameters for H_2 were then fitted in order to optimally reproduce the remaining interaction energy for all 1000 configurations. For the H_2-water interactions, water parameters were constrained to their value in the water-water interaction and only the H_2 parameters were changed. The resulting parameters for the H_2-water and H_2-H_2 interaction are listed in Table III together with the Boltzmann-weighted mean absolute error at 300 K for the fit to the 1000 configurations.

Bond potentials: For the water bond potential, the flexible Kumagai, Kawamura, and Yokokawa (KKY) potential model was used.[39] As was previously reported, the KKY potential parameters need to be reparametrized for correctly describing the water gas phase vibrational frequencies.[40] For the H_2 bond, a Morse potential has been fitted which reproduces the H_2 gas phase frequency of 4155 cm^{-1} at 200 K, using a timestep of 0.4 fs. The frequency shows a temperature dependence of about 4 cm^{-1}/100 K and a time step error.[41,42]

B. Classical and path integral MD simulations

Classical MD simulations: All MD simulations were carried out with both force field parametrizations (B3LYP/6-31G* and MP2/6-31G*) and a timestep of $\Delta t = 0.4$ fs, which allows flexible bonds in water and the H_2 molecules. The non-bonded interactions were truncated at a distance of 12 Å using a shift function for the electrostatic terms. For the model systems, simulations were carried out at 50 and 150 K using Langevin dynamics. After an initial equilibration of 50 ps, 100 snapshots separated by 1 ps were taken from the 100 ps production run. For the periodic systems, simulations were run at 50 and 150 K and at pressures of 1 and 1000 bars in the *NPT* ensemble using a Nose-Hoover thermostat with a coupling constant of 10 ps. After 100 ps of equilibration, 100 sets of coordinates separated by 1 ps were recorded for the calculation of the frequencies (*vide infra*).

TABLE III. LJ parameters for H_2 in H_2-water and H_2-H_2 interactions. The quality of the fit is reported as a Boltzmann-weighted mean absolute error of the fit to 1000 randomly generated configurations.

		$\sigma/2$ (Å)	ε (kcal/mol)	Fitting error (kcal/mol)
B3LYP/6-31G*	H_2-water	2.0051	−0.00100	0.0388
B3LYP/6-31G*	H_2-H_2	1.6075	−0.15993	0.0186
MP2/6-31G*	H_2-water	2.2870	−0.00050	0.0367
MP2/6-31G*	H_2-H_2	1.6330	−0.15912	0.0149

Path integral MD: Discretized Feynman path integral simulations[43,44] were used to capture quantum dynamical effects. The path integral module provided in the CHARMM program was used for this purpose.[30,45] Quantum dynamical simulations were carried out for the clathrate model systems using path integral MD. Simulations were carried out with 16 and 64 virtual particles (beads) using Langevin dynamics at the same temperatures used for the classical simulations. For the simulations with 64 beads, the timestep was reduced to 0.1 fs while the timestep of 0.4 fs was unchanged for the simulations with 16 beads. From each of the hundred coordinate sets of the PIMD simulations (separated by 1 ps from 100 000 PIMD evaluations), averages over the path positions were determined for each atom. These averaged structures were then used for the calculation of the vibrational frequencies.

C. Calculation of vibrational frequencies

Vibrational frequencies were calculated using DFT and MP2 electronic structure calculations. The coordinates obtained from the MD simulation with the parameter set corresponding to the given method were used as a starting point for the calculation. For the model systems, the inner water layer and the hydrogen molecules were included in the calculation. For the cages occupied by more than one hydrogen molecule, the frequency of one H_2 was calculated for each snapshot in the presence of the other H_2 molecules. For a specific snapshot, the frequencies of the different H_2 molecules in a given cage type differ. However, a comparison of the average frequency over 100 snapshots showed that the average frequency does not depend on which of the H_2 molecules was selected. For the periodic systems, one H_2 molecule was selected and the first water layer around it and hydrogens inside this layer were included in the calculation. The H_2 stretching potential was then determined for 5 distances corresponding to the minimum and the first and second classical turning points of the gas phase curve at the B3LYP/6-31G* or MP2/6-31G* level. A Morse potential was then fitted to the *ab initio* energies and the LEVEL[46] program was used to obtain the ground and first excited vibrational levels from which the frequency shift $\Delta\nu$ was calculated. Such a procedure was already successfully employed to assign structural substates in CO-ligated myoglobin.[47] This approach is also used when computing frequency trajectories $\omega(t)$ required for the analysis of 2DIR spectra.[48,49]

The reference vibrational frequency for free H_2 is at 4225 cm^{-1} for B3LYP/6-31G* and at 4299 cm^{-1} for MP2/6-31G*. In order to compare the results for different methods, the frequencies were scaled by the ratio of the experimental gas phase frequency of H_2 at 4155 cm^{-1} and the frequency of the respective electronic structure calculation method, resulting in scaling factors of 0.9834 for B3LYP/6-31G* and

0.9665 for MP2/6-31G*.[16] The combination of MD simulations and electronic structure calculations is required to obtain quantitatively correct frequency shifts of H_2 in clathrates. Calculating power spectra directly based on the H-H autocorrelation function yields redshifts of the H_2 in clathrates compared to free H_2 that are too small by about a factor of ten (i.e., they only show a few wavenumbers of redshift). Blueshifts are reproduced in quantitative agreement with electronic structure calculations. The reason for this is most likely the lack of polarization in the force field calculations.

III. RESULTS

A. Model systems

First, the findings for the clathrate model systems at $T = 50$ K are described. Vibrational frequencies obtained using B3LYP and MP2 calculations are compared and the results are reported in Figure 3. The vibrational frequencies cover a range from 4090 to 4190 cm^{-1} for both methods with the spectra from B3LYP calculations being slightly broader. In both cases, the lowest frequencies are found for a single H_2 molecule occupying the 5^{12} cage (S^1), with average frequencies of 4127 cm^{-1} for B3LYP and 4123 cm^{-1} for MP2. With two hydrogens in the 5^{12} cage (S^2), the average frequencies are at 4142 cm^{-1} for B3LYP and at 4150 cm^{-1} for MP2, respectively. Thus, the frequency difference between S^1 and S^2 almost doubles to 27 cm^{-1} for MP2 compared to 15 cm^{-1} for B3LYP.

Frequency differences between (S^1) and (L^1) calculated from B3LYP agree well with differences between (S^1) and (L^1) calculated from MP2. The average frequency for the L^1 cage is at 4145 cm^{-1} for B3LYP and at 4140 cm^{-1} for MP2, corresponding to differences between S^1 and L^1 of 18 and 17 cm^{-1}, respectively. For higher occupations of the $5^{12}6^4$ cage, average frequencies are 4148, 4152, and 4151 cm^{-1} for double (L^2), triple (L^3), and quadruple (L^4) occupations for B3LYP, compared to 4147, 4153, and 4155 cm^{-1} for MP2. Thus, for $5^{12}6^4$ cages, the frequency increase with higher H_2-occupation and approximately doubles for MP2 compared to B3LYP. Frequency increases between single and multiple occupation of 3, 7, and 6 cm^{-1} are found for B3LYP compared to 7, 13, and 15 cm^{-1} for MP2. In both cases, the increase is about equal between L^1 and L^2, while no or only a small increase is found between L^3 and L^4.

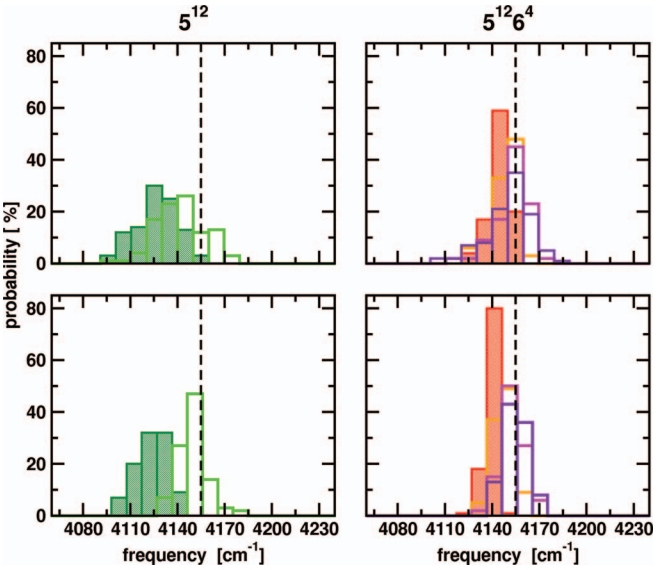

FIG. 3. Vibrational frequencies of clathrate model systems at 50 K. Upper panels: The B3LYP/6-31G* parametrization was used for the MD simulations in combination with B3LYP/6-31G* electronic structure calculations for the vibrational frequencies. Lower panel: The MP2/6-31G* parametrization was used for the MD simulations in combination with MP2/6-31G* electronic structure calculation for the vibrational frequencies. Color coding: 5^{12} cage with one (dark green) and two (light green) H_2 molecules; $5^{12}6^4$ cage with one (red), two (orange), three (magenta), and four (violet) H_2 molecules. The black lines show the frequency of free H_2 for comparison.

The results show that most of the computed frequencies and all frequency averages are shifted to the red with respect to free H_2 at 4155 cm^{-1}. The spectra can be compared to the experimental spectra and earlier studies on the basis of the frequency range and average frequencies for the two cavities. Since it is not evident whether the S^2 state exists at all in the experiments, the average of S^1 is used for the comparison of the 5^{12} cage and the average over L^1 to L^4 is used for the comparison for the $5^{12}6^4$ cage. For B3LYP, the frequency range extends from 4095 to 4185 cm^{-1}, with an average for S^1 at 4127 and averages over L^1 to L^4 at 4149 cm^{-1}. For MP2, the frequencies range from 4102 to 4170 cm^{-1} with averages for S^1 at 4123 cm^{-1} and for L^1 to L^4 at 4149 cm^{-1}. Compared to the experimental values at 99 K and 2000 bars[2] with a frequency range from 4112 to 4155 cm^{-1} and local maxima at 4119 and 4148 cm^{-1}, the calculated overall frequency range is too broad in both cases but in better agreement for MP2 than for B3LYP. For S^1, the averages are slightly too high compared to the experimental peak maxima, with again a better agreement for MP2. For L^1 to L^4, both computational approaches yield good agreement with experiment. Compared to earlier computational studies starting from minimized structures[16] with a frequency range between 4095 and 4177 cm^{-1} and maxima for S^1 at 4100 and for L^1 to L^3 at about 4125 cm^{-1}, the frequency ranges agree better with experiment for both methods and the frequency maxima are also clearly in better agreement from the present study with the experimentally observed peak maxima than the results for using optimized structures.[16] This indicates that optimizing the structures before the frequency calculation leads to artificially favorable positions of H_2 in the different clathrate cages and therefore to artificially low frequencies. The methods used here show slightly too small redshifts compared to experiment in contrast to considerably overestimated redshifts for earlier studies.[16] The difference with experiment is therefore much smaller in this study and underlines the importance of the thermal distribution of configurations as a starting point for the frequency calculations.

Configurational sampling versus electronic structure method: The difference between the results for the two approaches ([FF parametrization and sampling/frequency calculation] = [B3LYP/B3LYP] or [MP2/MP2]) can be further analyzed. Since both, the force field parametrization used for conformational sampling and the electronic structure calculation differ, the observations made above could arise

either from differences in the conformations sampled or due to differences in the electronic structure calculation methods. The two effects can be disentangled if the coordinates sampled from one parametrization (e.g., MP2) are used in frequency calculations using the other method (e.g., B3LYP), i.e., [MP2/B3LYP] in the notation above. The results are shown in Figure 4 in terms of average frequencies for the methods employed. Overall the data for the two sets of average frequencies with DFT electronic structure calculations look more similar than the evaluation with MP2, in particular the increase of vibrational frequency with higher cage occupation is very similar for the two sets of DFT results. The small difference between the two sets shows that the force field parameters also affect the final result, with differences of up to 5 cm^{-1}, but this effect is smaller than the differences between electronic structure calculations with differences up to 13 cm^{-1}. Such good agreement between two force fields may be partially due to the fact that small clathrate model systems are used with constraints on the outer layer of water molecules. However, it also shows that the accurate force field with atomic multipole moments and anharmonic bond potentials used in this study provides reliable results which are largely independent on the parametrization.

At this point it is useful to briefly consider potential pitfalls in the computational approaches used so far, specifically the question of coupling between individual H_2 molecules in the cage. For this, 10 arbitrary L^4 clusters were selected, the position of the H_2 molecules was frozen and their bond lengths were optimized. Then, harmonic frequencies were determined. It was found that in all cases the normal modes are localized on the individual H_2 molecules which suggests that there is little coupling of the vibrational modes. This justifies the procedure for calculating frequencies for individual H_2 molecules. This is also in accord with procedures to determine frequency trajectories in analyzing 2DIR spectroscopy where the solvent-solute coupling enters the calculation through the use of an effective potential.[48] In addition, we also considered the absolute frequencies when computed from normal mode calculations or scanning the energy along the H_2-bond and determining the frequency from solving the 1D Schrödinger equation for 10 snapshots of L^4. The correlation coefficient between the two sets of frequencies is 0.8 which is acceptable given that very different approximations are made in the two procedures.

1. Temperature effects

In order to assess the effect of temperature, all simulations were also carried out at 150 K. The results are compared based on the average frequency and are reported in Figure 5. It is found that typically the frequencies are higher at higher temperatures, however there is appreciable variation for different cage types and occupation numbers. The temperature dependent frequency increase is smallest for L^1 and L^2, with 1 and 2 cm^{-1} for B3LYP and 1 and 0 cm^{-1} for MP2. With increasing numbers of hydrogens in the $5^{12}6^4$ cage, temperature dependent frequency shifts increase and are 5 and 6 cm^{-1} for L^3 and L^4, respectively, for B3LYP, compared to 4 and 7 cm^{-1} for MP2. For the 5^{12} cages, the temperature dependent frequency shift is larger, with 6 cm^{-1} for S^1 with both methods and 37 and 39 cm^{-1} for S^2 with B3LYP and MP2, respectively. Overall, the agreement between the different calculation methods is very good here and the evaluation demonstrates that 5^{12} cages are more sensitive to temperature effects than $5^{12}6^4$ cages and the temperature effect is also more pronounced at higher cage occupation numbers.

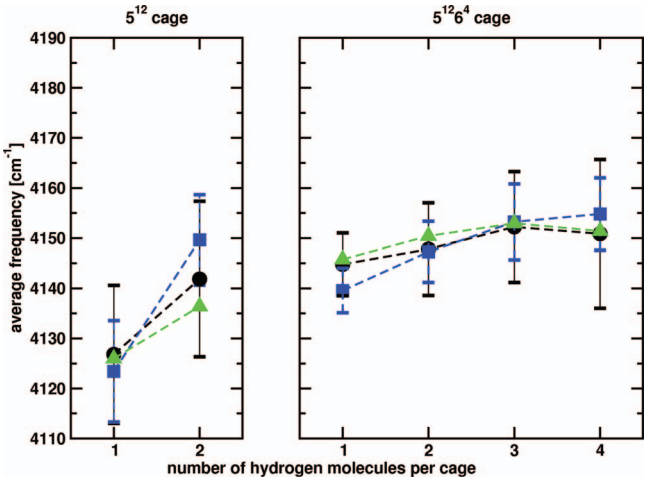

FIG. 4. Comparison of effects of the force field compared to effects of the electronic structure calculation method. Black circles show the average frequencies for B3LYP/6-31G* parametrization in MD simulations in combination with B3LYP/6-31G* electronic structure calculations, blue squares show the results for MP2/6-31G* parametrization and MP2/6-31G* electronic structure calculation, and green triangles show the combination of the MP2/6-31G* parametrization with B3LYP/6-31G* electronic structure calculations. The error bars show the standard deviation for the corresponding sets.

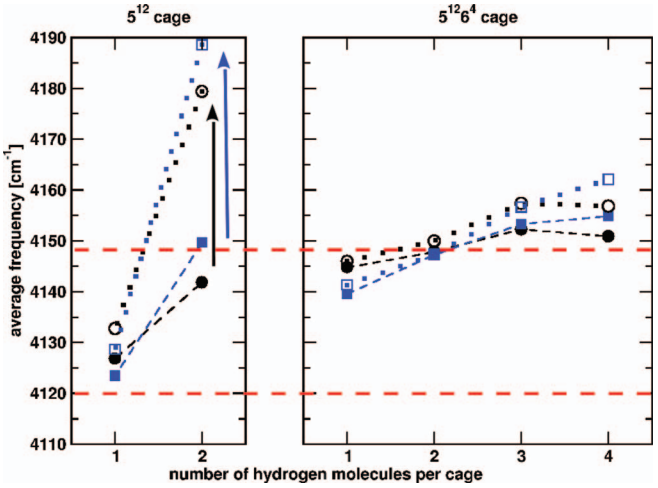

FIG. 5. Average vibrational frequencies of clathrate model systems at 50 K and 150 K. Circles show the average frequencies for B3LYP/6-31G* parametrization in MD simulations in combination with B3LYP/6-31G* electronic structure calculations. Squares show the results for MP2/6-31G*. Filled symbols and dashed lines represent results at 50 K, open symbols and dotted lines represent results at 150 K. The red lines are the experimental peak maxima at 2000 bars and 99 K.[2]

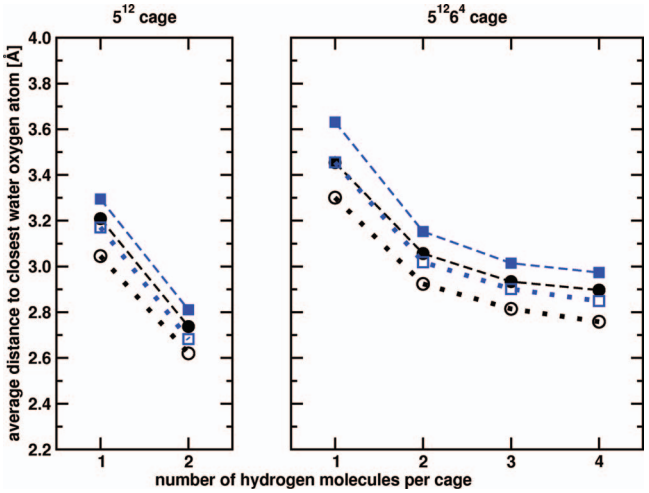

FIG. 6. Evaluation of the closest distance between a water oxygen atom and a H_2 atom in the different clathrate cages. The results from of the B3LYP/6-31G* parametrization (black symbols) are compared to the results from the MP2/6-31G* parametrization (blue symbols) at 50 K (filled symbols and dashed lines) and 150 K (open symbols and dotted lines).

2. Structure-frequency relationships

To correlate structure and frequency shifts, the closest distance between a H_2 molecule and a water oxygen atom of the clathrate is evaluated. The results reported in Figure 6 show that lower frequencies correlate with larger distances to the closest water-oxygen atom.

In addition to the distances between H_2 molecules and the water oxygen atom, the effect of the different clathrate environments on the rotational dynamics of H_2 molecules is considered. For this, H_2-rotational reorientation times (τ_l) were calculated according to[50]

$$C_l(t) = \langle P_l(\mathbf{u}(0) \cdot \mathbf{u}(t)) \rangle. \quad (2)$$

Here, $C_l(t)$ is the rotational correlation function, P_l is the Legendre polynomial of order l, and $\mathbf{u}(t)$ is the unit vector pointing along the H_2 axis. It was found that $C_l(t)$ can be well approximated by a single exponential decay ($C_l(t) \approx e^{-l(l+1)D_R t}$). The rotational correlation time τ_2 can therefore be obtained by fitting to an exponential function $C_2(t) = ae^{-t/\tau_2} + c$.[50] The rotational correlation times for the MP2 parametrization are shown in Table IV at 50 K and 150 K. Overall, the rotational correlation times are longer at lower temperatures as expected. The differences between different cage types are generally small, with the exception of S^2 at 50 K, where τ_2 is about five times larger than for the other cage types at this temperature. τ_2 is also largest for S^2 at 150 K, but in this case the effect is very small. The fastest reorientation times are found for S^1 at both temperatures. The increase of τ_2 in going from S^1 to L^1 is most likely due to the fact that in S^1 the H_2 molecule remains at the center of the cage and rotates freely, whereas in L^1 it moves between different sites within the cage and undergoes specific favorable interactions with individual water molecules. These specific interactions are weaker if more H_2 molecules are present in the case of L^4. The large value of τ_2 for S^2 can be explained by the fact that there are only very few positions and orientations that allow a favorable interaction of two H_2 molecules in the 5^{12} cage. The very slow rotation at 50 K preserves these favorable interactions, whereas they disappear at 150 K due to conformational sampling. The lack of favorable interactions at 150 K for S^2 is in agreement with the blueshifted frequencies, in contrast to redshifts at 50 K.

TABLE IV. Rotational correlation times τ_2 in ps for H_2 using MP2/6-31G* data from model systems.

	τ_2 (ps)	
Cage type	50 K	150 K
S^1	0.0411	0.0241
S^2	0.2510	0.0306
L^1	0.0510	0.0300
L^4	0.0438	0.0253

3. Quantum effects

Calculations with the same two parameter sets have been carried out using path integral MD simulations with 16 and 64 beads at 50 and 150 K. From these simulations, average structures over all path points are calculated and used for the calculation of vibrational frequencies. Average structures and the path distribution at 50 and 150 K are shown in Figure 7.

The use of average structures for the calculation of vibrational frequencies does not include a direct evaluation of the quantum dynamical vibrational spectrum which is computationally too expensive due to its unfavorable numerical convergence properties.[51,52] Instead, quantum dynamical effects on the vibrational frequencies are included in an average fashion which does not allow to evaluate dynamical

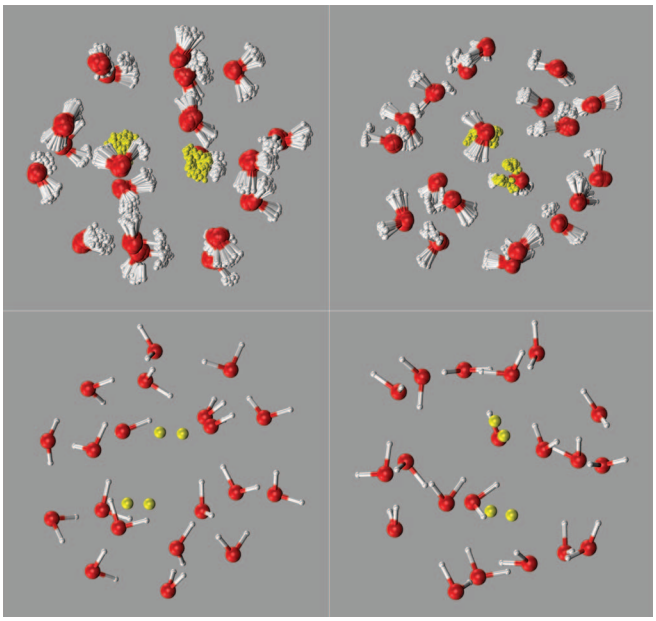

FIG. 7. Average structures (bottom) and path distributions (top) from PIMD simulations at 50 K (left) and at 150 K (right). The structures are for an S^2 clathrate cage with the hydrogen molecules shown as yellow points.

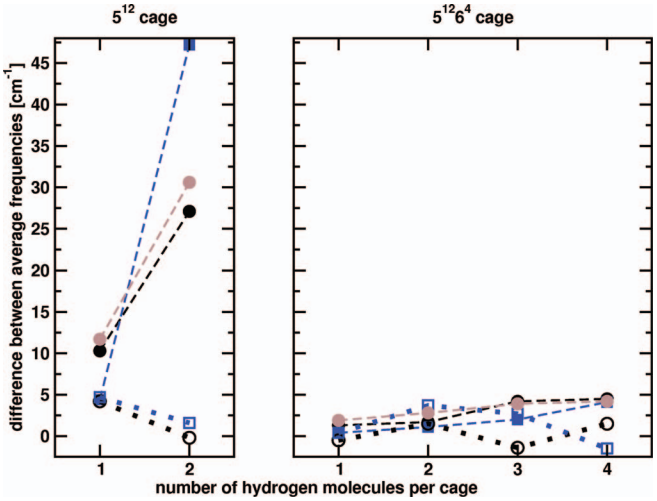

FIG. 8. Differences in the average vibrational frequencies between classical and path integral MD simulations for the clathrate model systems at 50 K and 150 K. Black circles show the differences between averages frequencies for the B3LYP/6-31G* setup and blue squares show the results for MP2/6-31G*. The differences are calculated for blue and black lines between a path integral simulation with 64 beads and the corresponding classical simulation. The brown lines show the differences to simulations with 16 beads at 50 K for the B3LYP setup. Filled symbols and dashed lines represent results at 50 K and open symbols and dotted lines represent results at 150 K.

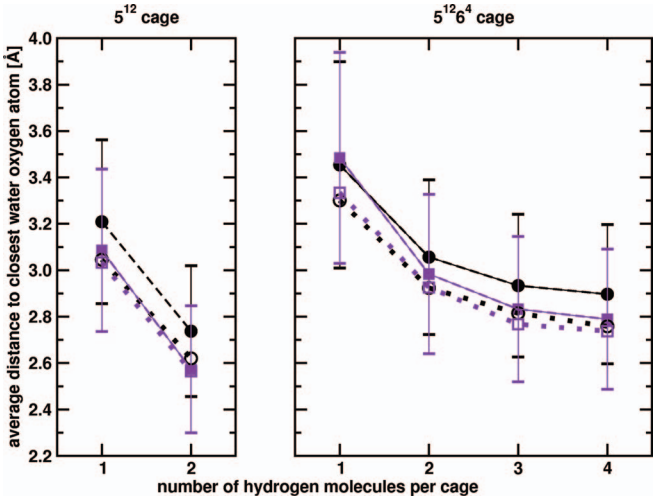

FIG. 9. Evaluation of the closest distance between a water oxygen atom and a H_2 atom in the different clathrate cages. The results from classical simulations (black symbols) are compared to the results from PIMD simulations with 64 beads (violet symbols) at 50 K (filled symbols and dashed lines) and 150 K (open symbols and dotted lines). The B3LYP/6-31G* parametrization is used for this evaluation. The error bars show the standard deviation for the corresponding sets.

correlation effects of atoms, but it includes effects related to changes in the average structure and the distribution of hydrogen positions inside the clathrate. The results from the classical simulations of the model systems are compared to results from PIMD simulations in Figure 8. The differences $\omega_C - \omega_Q$ between the average frequencies of the classical simulations ω_C and the PIMD simulations ω_Q are shown at 50 and 150 K for both force fields. In general, 64 beads are used for the PIMD simulations. A comparison to a setup with 16 beads is shown in Figure 8 for a simulation at 50 K and the results are very similar to the corresponding calculations with 64 beads. The evaluation shows that in general, the differences between quantum and classical simulation are larger at 50 K, as expected. The 5^{12} cages appear to be far more affected by quantum dynamical effects than the $5^{12}6^4$ cages, in particular for S^2. For the $5^{12}6^4$ cages, the effects are within a few wavenumbers and increase slightly with increasing numbers of hydrogens. For simulations at 50 K, the quantum effects generally lead to higher frequencies, while at 150 K, some frequency reductions due to quantum effects are observed, in particular for larger numbers of hydrogens in the $5^{12}6^4$ cage. The overall effect of this is that the results at 50 K and 150 K become more similar due to quantum effects, which is in agreement with experimental spectra showing only a small and gradual change of the peak positions with temperature.[5]

In order to understand the origin of the difference in vibrational frequencies between the classical and PIMD simulations, the structural differences between the snapshots obtained from the classical MD simulations and the path averaged structures from the PIMD simulations have been analyzed. It was found that the structural differences can be characterized by evaluating the closest distance between a H_2 molecule and a water oxygen atom in the different clathrate cage types. The averages and standard deviations over all snapshots are shown in Figure 9. In general, the distances between each H of any H_2 molecule and the water oxygen atom closest to it are shorter for the 5^{12} cage than for the $5^{12}6^4$ cage and decrease with increasing numbers of H_2 molecules per cage as expected. The comparison between the classical and the path integral simulations shows that at 50 K the distances of the path integral simulations are systematically shorter than the distances of the classical simulations, with the exception of the L^1 cage where the results for classical and quantum simulations are similar. At 150 K, the differences between classical and PIMD simulations are small. The effect of increasing the temperature from 50 to 150 K is similar to the quantum dynamical effects, which is in agreement with the changes in vibrational frequencies.

B. Periodic systems

The results discussed so far have all been obtained from calculations on clathrate model systems. These model systems include only the first and second water layer around the H_2 molecules in different clathrate cages and therefore do not capture effects from molecules at larger distances or effects from the collective motion of clathrate molecules, e.g., lattice vibrations. In order to assess these influences, simulations with periodic systems have been carried out and are compared to the results for the model systems. In the following, different force field parametrizations, fractions of H_2 in the clathrate and temperatures and pressures are considered. The average volumes obtained for different pressures, temperatures, and H_2 fractions during the MD simulations in the *NPT* ensemble are shown in Figure 10 and find a steady increase of the box volume with increasing H_2 fractions, increasing temperatures, and pressures. At 50 K, the system is stable with all hydrogen loads, with unit cell parameters ranging from 16.8

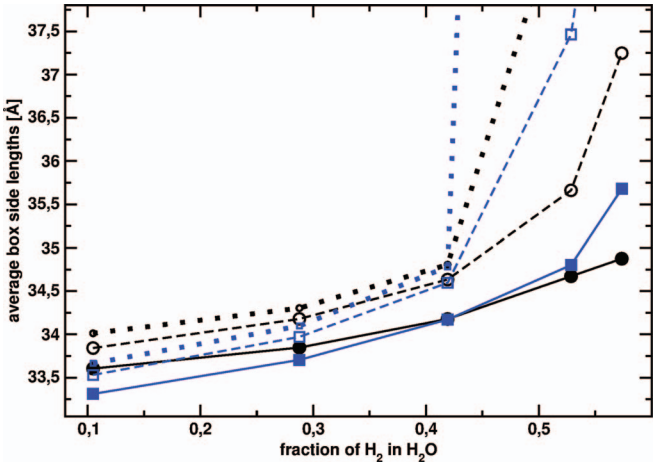

FIG. 10. Comparison of average simulation box volume in *NPT* simulation for different fractions of H_2 in the clathrate, different force field parameters, and different temperatures and pressures. Black circles represent simulations with force field parameters obtained from B3LYP/6-31G* calculations and blue squares represent parametrization based on MP2/6-31G* calculations. Filled symbols and solid lines represent results at 50 K and 1000 bars, open symbols and dashed lines represent results at 150 K and 1000 bars, and small open symbols and dotted lines represent results at 150 K and 1 bar.

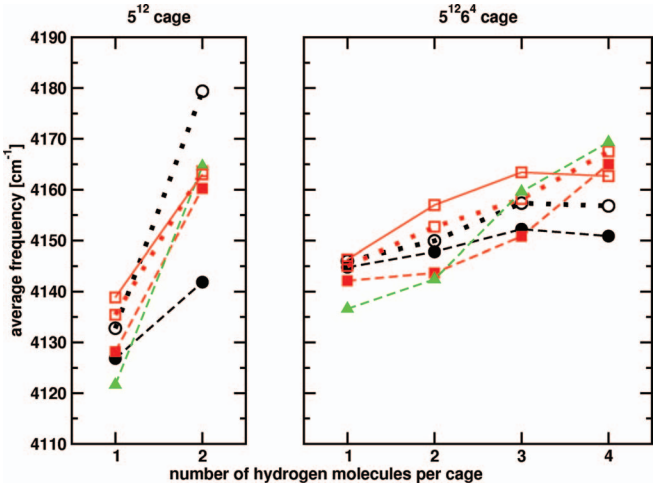

FIG. 11. Comparison of the frequencies obtained based on simulations with periodic clathrate setups and model systems at 50 and 150 K. The results for the model systems are shown as black circles and the results for the periodic systems are shown as red squares and green triangles. The red squares represent simulations done with the B3LYP parameters and the green triangles represent simulations with the MP2 parameters. Filled symbols and dashed lines represent results at 50 K and 1000 bars, open symbols and dotted lines represent results at 150 K and 1000 bars, and open symbols and solid lines represent results at 150 K and 1 bar. (Pressures are only relevant for the periodic systems.)

to 17.4 Å for the B3LYP parametrized force field and from 16.7 to 17.8 Å for the MP2 parametrized force field. At 150 K, the system is not stable anymore with the largest fractions of H_2 (box side length values of more than 37 Å in Figure 10 correspond to melting of the clathrate; the box side length is twice the unit cell side length), which is in agreement with experiments which show that clathrates are stable with H_2:H_2O fractions of up to 1:2.[2] For the stable clathrates at 150 K and 1000 bars, unit cell volumes range between 16.9 and 17.8 Å for the B3LYP parametrized force field and from 16.8 to 17.3 Å for MP2 parameters. The simulations at 150 K and 1 bar show slightly larger volumes and faster dissociation. In general, the simulations with B3LYP parameters show a slightly lower dependence of the box volume on the H_2 fraction and temperature, however, overall differences between the two parametrizations are small and the unit cell side lengths is in both cases in good agreement with the experimental unit cell side lengths of 17 Å at 100 K.[2]

For the calculation of the frequencies, water and hydrogen molecules corresponding to the two different clathrate cage types and occupation numbers are selected from the configurations of the periodic system. The number of molecules included in the electronic structure calculation is equal to the number of molecules used in the model system for the corresponding cage type and occupation number. The frequencies for S^1, L^1, and L^2 are calculated based on the simulations with the lowest hydrogen fraction of 10.48%. For L^3 and L^4, the setup with 28.77% of H_2 is used and S^2 is taken from the simulation with 41.91% of hydrogen. The results are shown in Figure 11 and compared to the model systems. Since different force field parameters can have a larger effect for the periodic system than for the model system, both force field parametrizations are used and compared in combination with electronic structure calculations at the B3LYP/6-31G* level. The overall findings are similar to the results for the model systems. The only notable difference between the model system and the periodic system is found for S^2: the frequency change is larger by 17 cm^{-1} for the periodic systems compared to the model system at 50 K and smaller by 18 cm^{-1} at 150 K. In other words, the frequency change with temperature is much smaller in the periodic system than in the model system. For the $5^{12}6^4$ cage, frequencies are slightly lower for L^1. The increase with additional hydrogens depends on the pressure. In the simulations at 1000 bars, the frequencies increase more rapidly and more linearly with additional hydrogens than in the model systems, in particular in the simulations with the MP2 parameters. The simulation at 1 bar shows in contrast a similar pattern of the frequency change with additional H_2 molecules as in the model systems, with a slight decrease in frequency between L^3 and L^4. It can therefore be concluded that the frequency is not necessarily a linear function of the number of H_2 molecules, the change in frequency is pressure dependent and more pronounced at high pressures, which is in contrast to findings in earlier studies which are based on optimized structures and suggest generally a linear correlation between the frequency and the number of neighboring H_2 molecules.[16]

IV. DISCUSSION AND CONCLUSIONS

In this study, a combination of computational strategies has been used to calculate vibrational frequencies of H_2 molecules in clathrate hydrates and to relate them with occupation numbers of the different clathrate cage types. In contrast to earlier studies, the effects of temperature, pressure, and quantum dynamical effects were included in the simulations. This provided the necessary data to make direct contact with experimental data. In particular, the frequency ranges

over which the H_2 vibrations are distributed, agree favorably with experiment.[2,5–7] The changes of the vibrational frequencies with temperature were evaluated and the importance of quantum dynamical effects on the vibrational frequencies was assessed for different clathrate environments. Furthermore, the performance of different force field parametrizations and electronic structure calculation methods were compared.

It was found that for different force fields and at different temperatures, the lowest frequencies are observed for H_2 in the singly occupied 5^{12} cage. The frequency is higher for the singly occupied $5^{12}6^4$ cage and increases with increasing cage occupation numbers. While these general findings are the same for force field parametrizations based on B3LYP/6-31G* and MP2/6-31G*, the increase of vibrational frequency with additional H_2 molecules per cage is approximately twice as large for MP2/6-31G* electronic structure based on the same structures. Overall, the trends for different clathrate environments are comparable to earlier studies,[16] with the singly occupied 5^{12} cage showing the largest redshift and a reduction of the redshift with increasing numbers of hydrogen molecules per cage. While frequency shifts of other clathrates can be rationalized in terms of the loose cage-tight cage model,[21,22] this model explains only parts of the frequency shifts in H_2 clathrates: a loose cage situation with a favorable interaction between the guest molecule and the cage wall is clearly found for S^1 and L^1-L^2. Additional H_2 molecules are shifting the frequencies according to a tight cage situation with unfavorable guest-host interactions, this gradually reduces the frequency shift. However, the loose cage-tight cage model cannot directly explain the difference between S^1 and L^1. The change of frequency with additional hydrogens per cage depends on temperature, pressure and quantum dynamical effects and is not necessarily a linear function of the number of hydrogen molecules. We found that the 5^{12} cage is more sensitive to the details of the environment and to quantum dynamical effects, in particular when it is doubly occupied. While the frequency of the doubly occupied 5^{12} cage in the model system at 50 K is redshifted by -5 and -13 cm^{-1} with B3LYP/6-31G* and MP2/6-31G*, respectively, it is observed in the blueshifted frequency range in all calculations with the periodic systems. Furthermore, the frequency is found to increase due to quantum dynamical effects. For these reasons it is unlikely that hydrogen clathrates contain a substantial amount of doubly occupied 5^{12} cages, since this would probably result in a separate, blueshifted peak, which has not been observed experimentally so far. For clathrates it is therefore more likely that the $5^{12}6^4$ cages contain larger numbers of H_2. The increase of vibrational frequency with increasing H_2 occupation in the $5^{12}6^4$ cages is much smaller than for the 5^{12} cages and can be reduced further by quantum dynamical effects. As a consequence, a large fraction of hydrogen located mainly in the $5^{12}6^4$ clathrate cages would result in two peaks in the H_2 Raman spectrum, a small peak with a large redshift corresponding to the singly occupied 5^{12} cages and a much larger and only slightly redshifted peak corresponding to high occupations of the $5^{12}6^4$ cages, which is how the Raman spectrum of hydrogen clathrate appears at high H_2 pressures.[2]

ACKNOWLEDGMENTS

The authors wish to acknowledge helpful discussions with Dr. Mike Devereux and Dr. Tristan Bereau about the frequency calculation and the parameter fitting. Financial support from the Swiss National Science Foundation through Grant No. 200021-117810 and the NCCR-MUST is gratefully acknowledged.

[1] H. Lee, J.-W. Lee, D. Y. Kim, J. Park, Y.-T. Seo, H. Zeng, I. L. Moudrakovski, C. I. Ratcliffe, and J. A. Ripmeester, Nature **434**, 743 (2005).
[2] W. L. Mao, H. Mao, A. F. Goncharov, V. V. Struzhkin, J. Guo, Q. Hu, J. Shu, R. J. Hemley, M. Somayazulu, and Y. Zhao, Science **297**, 2247 (2002).
[3] T. C. W. Mak and R. K. McMullan, J. Phys. Chem. **42**, 2732 (1965).
[4] S. Patchkovskii and J. S. Tse, Proc. Natl. Acad. Sci. U.S.A. **100**, 14645 (2003).
[5] A. Giannasi, L. Celli, M. Ulivi, and M. Zoppi, J. Chem. Phys. **129**, 084705 (2008).
[6] T. A. Strobel, K. C. Hester, C. A. Koh, A. K. Sum, and E. D. Sloan, Chem. Phys. Lett. **478**, 97 (2009).
[7] T. A. Strobel, E. D. Sloan, and C. A. Koh, J. Chem. Phys. **130**, 014506 (2009).
[8] W. L. Mao and H. K. Mao, Proc. Natl. Acad. Sci. U.S.A. **101**, 708 (2003).
[9] T. A. Strobel, C. A. Koh, and D. E. Sloan, Fluid Phase Equilib. **261**, 382 (2007).
[10] F. Schotte, M. Lim, T. A. Jackson, A. V. Smirnov, J. Soman, J. Olson, G. Phillips, M. Wulff, and P. Anfinrud, Science **300**, 1944 (2003).
[11] N. Plattner and M. Meuwly, Biophys. J. **94**, 2505 (2008).
[12] N. Plattner, M. W. Lee, and M. Meuwly, Faraday Discuss. **147**, 217 (2010).
[13] K. Nienhaus, S. Lutz, M. Meuwly, and G. U. Nienhaus, ChemPhysChem **11**, 119 (2010).
[14] S. Alavi, J. A. Ripmeester, and D. D. Klug, J. Chem. Phys. **123**, 024507 (2005).
[15] S. Alavi, D. D. Klug, and J. A. Ripmeester, J. Chem. Phys. **128**, 064506 (2008).
[16] J. Wang, H. Lu, J. A. Ripmeester, and U. Becker, J. Phys. Chem. C **114**, 21042 (2010).
[17] M. Xu, Y. S. Elmatad, F. Sebastianelli, J. W. Moskowitz, and Z. Bacic, J. Phys. Chem. B **110**, 24806 (2006).
[18] F. Sebastianelli, M. Xu, Y. S. Elmatad, J. W. Moskowitz, and Z. Bacic, J. Phys. Chem. C **111**, 2497 (2007).
[19] M. Xu, F. Sebastianelli, and Z. Bacic, J. Phys. Chem. A **113**, 7601 (2009).
[20] P. M. Felker, J. Chem. Phys. **138**, 174306 (2013).
[21] G. C. Pimentel and S. W. Charles, Pure Appl. Chem. **7**, 111 (1963).
[22] H. Schober, H. Itoh, A. Klapproth, V. Chiaia, and W. F. Kuhs, Eur. Phys. J. E **12**, 41 (2003).
[23] K. R. Ramya, G. V. P. Kumar, and A. Venkatnathan, J. Chem. Phys. **136**, 174305 (2012).
[24] K. R. Ramya and A. Venkatnathan, J. Chem. Phys. **138**, 124305 (2013).
[25] A. Witt, F. Sebastianelli, M. E. Tuckerman, and Z. Bacic, J. Phys. Chem. C **114**, 20775 (2010).
[26] N. Plattner and M. Meuwly, ChemPhysChem **9**, 1271 (2008).
[27] N. Plattner, T. Bandi, J. D. Doll, D. L. Freeman, and M. Meuwly, Mol. Phys. **106**, 1675 (2008).
[28] M. W. Lee, N. Plattner, and M. Meuwly, Phys. Chem. Chem. Phys. **14**, 15464 (2012).
[29] B. R. Brooks, R. E. Bruccoleri, B. D. Olafson, D. J. States, S. Swaminathan, and M. Karplus, J. Comput. Chem. **4**, 187 (1983).
[30] B. R. Brooks, C. L. Brooks III, L. Nilsson, R. J. Petrella, B. Roux, Y. Won, G. Archontis, C. Bartels, S. Boresch, A. Caflisch *et al.*, J. Comput. Chem. **30**, 1545 (2009).
[31] A. J. Stone, *The Theory of Intermolecular Forces* (Clarendon Press, Oxford, 1996).
[32] A. J. Stone, J. Chem. Theor. Comput. **1**, 1128 (2005).
[33] M. J. Frisch, G. W. Trucks, H. B. Schlegel *et al.*, Gaussian 03, Revision C.02, Gaussian, Inc., Wallingford, CT, 2004.
[34] W. L. Jorgensen, J. D. Chandrasekhar, J. D. Madura, R. W. Impey, and M. L. Klein, J. Chem. Phys. **79**, 926 (1983).
[35] C. Kramer, P. Gedeck, and M. Meuwly, J. Chem. Theor. Comput. **9**, 1499 (2013).

[36]A. Warshel and S. Lifson, J. Chem. Phys. **53**, 582 (1970).
[37]H. Heinz, R. A. Vaia, B. L. Farmer, and R. R. Naik, J. Phys. Chem. C **112**, 17281 (2008).
[38]S. Simon, M. Duran, and J. J. Dannenberg, J. Chem. Phys. **105**, 11024 (1996).
[39]N. Kumagai, K. Kawamura, and T. Yokokawa, Mol. Simul. **12**, 177 (1993).
[40]C. J. Burnham, J. C. Li, and M. Leslie, J. Phys. Chem. B **101**, 6192 (1997).
[41]P. Berens and K. R. Wilson, J. Chem. Phys. **74**, 4872 (1981).
[42]J. Danielsson and M. Meuwly, J. Phys. Chem. B **111**, 218 (2007).
[43]D. Chandler and P. G. Wolynes, J. Chem. Phys. **74**, 4078 (1981).
[44]M. E. Tuckerman, B. J. Berne, G. J. Martyna, and M. L. Klein, J. Chem. Phys. **99**, 2796 (1993).
[45]K. Hinsen and B. Roux, J. Phys. Chem. **106**, 3567 (1997).
[46]R. J. Le Roy, Chem. Phys. Res. Report No. CP–555R, 1996.
[47]M. Meuwly, Chem. Phys. Chem. **7**, 2061 (2006).
[48]S. Li, J. Schmidt, S. Corcelli, C. Lawrence, and J. Skinner, J. Chem. Phys. **124**, 204110 (2006).
[49]M. W. Lee, J. Carr, M. Gollner, P. Hamm, and M. Meuwly, J. Chem. Phys. **139**, 054506 (2013).
[50]J. E. Adams and A. Siavosh-Haghighi, J. Phys. Chem. B **106**, 7973 (2002).
[51]D. Thirumalai and B. J. Berne, Comput. Phys. Commun. **63**, 415 (1991).
[52]J. D. Doll, T. L. Beck, and D. L. Freeman, J. Chem. Phys. **89**, 5753 (1988).